J Mol Neurosci (2013) 51:602–614
DOI 10.1007/s12031-013-0033-5

Increased TRPV4 Expression in Urinary Bladder and Lumbosacral Dorsal Root Ganglia in Mice with Chronic Overexpression of NGF in Urothelium

Beatrice M. Girard · Liana Merrill · Susan Malley · Margaret A. Vizzard

Received: 15 April 2013 / Accepted: 9 May 2013 / Published online: 21 May 2013

Abstract Transient receptor potential vanilloid (TRPV) family member 4 (TRPV4) expression has been demonstrated in urothelial cells and dorsal root ganglion (DRG) neurons, and roles in normal micturition reflexes as well as micturition dysfunction have been suggested. TRP channel expression and function is dependent upon target tissue expression of growth factors. These studies expand upon the target tissue dependence of TRPV4 expression in the urinary bladder and lumbosacral DRG using a recently characterized transgenic mouse model with chronic overexpression of nerve growth factor (NGF-OE) in the urothelium. Immunohistochemistry with image analyses, real-time quantitative polymerase chain reaction, and Western blotting were used to determine TRPV4 protein and transcript expression in the urinary bladder (urothelium + suburothelium, detrusor) and lumbosacral DRG from littermate wild-type (WT) and NGF-OE mice. Antibody specificity controls were performed in TRPV4$^{-/-}$ mice. TRPV4 transcript and protein expression was significantly ($p \leq 0.001$) increased in the urothelium + suburothelium and suburothelial nerve plexus of the urinary bladder and in small- and medium-sized lumbosacral (L1, L2, L6-S1) DRG cells from NGF-OE mice compared to littermate WT mice. NGF-OE mice exhibit significant ($p \leq 0.001$) increases in NGF transcript and protein in the urothelium + suburothelium and lumbosacral DRG. These studies demonstrate regulation of TRPV4 expression by NGF in lower urinary tract tissues. Ongoing studies are characterizing the functional roles of TRPV4 expression in the sensory limb (DRG, urothelium) of the micturition reflex.

B. M. Girard · L. Merrill · S. Malley · M. A. Vizzard (✉)
Department of Neurological Sciences, University of Vermont College of Medicine, D415A Given Research Building, Burlington, VT 05405, USA
e-mail: margaret.vizzard@uvm.edu

Keywords Micturition · Sensory transducer · Growth factor · Q-PCR · Western blot

Introduction

Bladder pain syndrome (BPS)/interstitial cystitis (IC) is one type of chronic pain syndrome characterized by pain, pressure or discomfort perceived to be bladder related with at least one urinary symptom (Hanno et al. 2010). A recent study concluded that 3.3–7.9 million women (>18 years old) in the USA exhibit BPS/IC symptoms (Berry et al. 2011). The impact of BPS/IC on quality of life is enormous, and the economic burden is significant (Clemons et al. 2002). Although the etiology and pathogenesis of BPS/IC are unknown, numerous theories including infection, inflammation, autoimmune disorder, toxic urinary agents, urothelial dysfunction, and neurogenic causes have been proposed (Petrone et al. 1995; Ho et al. 1997; Johansson et al. 1997; Driscoll and Teichman 2001; Sant and Hanno 2001). We have hypothesized that pain associated with BPS/IC involves an alteration of visceral sensation/bladder sensory physiology. Altered visceral sensations from the urinary bladder (i.e., pain at low or moderate bladder filling) that accompany BPS/IC (Petrone et al. 1995; Ho et al. 1997; Johansson et al. 1997; Driscoll and Teichman 2001; Sant and Hanno 2001) may be mediated by many factors including changes in the properties of peripheral bladder afferent pathways such that bladder afferent neurons respond in an exaggerated manner to normally innocuous stimuli (allodynia). These changes may be mediated, in part, by inflammatory changes in the urinary bladder. Neurotrophins (e.g., nerve growth factor, NGF) have been implicated in the peripheral sensitization of nociceptors (Lindsay and Harmar 1989; Dray 1995; Dinarello 1997). Intravenous administration of a humanized monoclonal antibody that specifically inhibits

NGF (tanezumab) in patients with BPS/IC demonstrates proof of concept by improving the global response assessment and reducing the urgency episode frequency (Evans et al. 2011). However, clinical trials involving systemic anti-NGF therapies for diverse pain conditions have halted enrollment due to incidence and risk of osteonecrosis (Seidel and Lane 2012). The need for additional lower urinary tract (LUT) targets beyond NGF is clear.

The transient receptor potential (TRP) channels are a novel superfamily of non-specific ion channels with high Ca^{2+} permeability (Everaerts et al. 2010; Moran et al. 2011). Multiple TRP channels are expressed in the urinary bladder and may act as sensors of stretch and/or chemical irritation in the LUT (Andersson et al. 2010; Araki 2011; Eid 2011). Involvement of TRP channels in normal micturition reflex function as well as micturition dysfunction has been suggested (Andersson et al. 2010; Araki 2011; Eid 2011). Studies of TRP channels in the LUT have primarily focused on TRP ankyrin (TRPA) family member 1 (TRPA1), TRP vanilloid family member 1 (TRPV1) or 4 (TRPV4) and functional roles (Andersson et al. 2010) in overactive bladder and BPS/IC have been suggested (Nilius et al. 2007; Everaerts et al. 2008). The focus of these studies is on the vanilloid (TRPV) family member TRPV4 because previous studies (Everaerts et al. 2008) have reported very low levels of TRPA1 and TRPV1 mRNA but high levels of TRPV4 mRNA in urothelial cells consistent with our recent studies (Merrill et al. 2012b). Previous studies have demonstrated that TRP channel function and modulation in sensory neurons is dependent upon target tissue expression of growth factors (e.g., glial-derived neurotrophic factor (GDNF) (Malin et al. 2011). The current studies expand upon the target tissue dependence of TRPV channel expression (Malin et al. 2011) by examining TRPV4 expression in urinary bladder and lumbosacral dorsal root ganglia (DRG) in a transgenic mouse model with chronic NGF overexpression (NGF-OE) in the urothelium (Cheppudira et al. 2008; Schnegelsberg et al. 2010; Girard et al. 2011, 2012).

Materials and Methods

Animals

NGF-OE mice: NGF-OE transgenic mice were generated at Roche Palo Alto (material transfer agreement with Roche Palo Alto and Dr. Debra Cockayne) in collaboration with Dr. Henry Sun at New York University Medical School as previously described (Cheppudira et al. 2008; Schnegelsberg et al. 2010). Animal genotype was confirmed by Southern and/or PCR analyses; all mice have the inbred genetic C57BL/6J background and were derived from F2 to F4 generations maintained through a hemizygous backcross strategy with C57BL/6J wild-type (WT) mice. Mice used in this study were bred locally at The University of Vermont College of Medicine. The litters were of normal size, and weight and behaviors (feeding, drinking, activity patterns) appeared normal. Littermate WT mice were used as controls throughout these studies. All experimental protocols involving animal use were approved by the University of Vermont (UVM) Institutional Animal Care and Use Committee. Animal care was under the supervision of the UVM Office of Animal Care Management in accordance with the Association for Assessment and Accreditation of Laboratory Animal Care and National Institutes of Health guidelines.

Measurement of Urinary Bladder and Lumbosacral DRG NGF by ELISAs

NGF content in the urinary bladder and lumbosacral DRG of NGF-OE transgenic mice and WT littermate controls was determined using enzyme-linked immunoassays as previously described (Vizzard 2000; Cheppudira et al. 2008; Schnegelsberg et al. 2010). Individual bladders and DRG were weighed and solubilized in tissue protein extraction agent (T-PER; Roche, Indianapolis, IN), a mild zwitterionic dialyzable detergent in 25 mM bicine, 150 mM sodium chloride (pH 7.6) supplemented with a protease inhibitor mix (16 μg/ml benzamidine, 2 μg/ml leupeptin, 50 μg/ml lima bean trypsin inhibitor, and 2 μg/ml pepstatin A, Sigma-Aldrich), and aliquots were removed for protein assays. Tissue was homogenized using a Polytron homogenizer, centrifuged (10,000 rpm for 10 min), and the resulting supernatant was used for NGF protein quantification. Total protein was determined using the Coomassie Plus Protein Assay Reagent Kit (Thermo Fischer Scientific, Rockford, IL). Microtiter plates (R&D Systems, Minneapolis, MN) were coated with a mouse anti-rat NGF antibody (R&D Systems, Minneapolis, MN). Sample and standard solutions were run in duplicate. A horseradish peroxidase-streptavidin conjugate was used to detect the antibody complex. Tetramethyl benzidine was the substrate, and the enzyme activity was measured by the change in optical density. The NGF standard provided with this protocol generated a linear standard curve from 15 to 1,000 pg/ml (R^2=0.998, $P \leq$ 0.0001) for tissue samples. The absorbance values of standards and samples were corrected by subtraction of the background absorbance due to nonspecific binding. No samples fell below the minimum detection limits of the assay, and no samples were diluted prior to use. Curve fitting of standards and evaluation of NGF content of samples were performed using a least squares fit as previously described (Vizzard 2000; Schnegelsberg et al. 2010).

Littermate WT and NGE-OE (n=7–9 for each) female mice were deeply anesthetized with isoflurane (4 %) and then euthanized via thoracotomy. The urinary bladder and lumbosacral (L1, L2, L5-S1) DRG were quickly dissected

under RNase-free conditions. In some instances, the bladder was cut open along the midline and pinned to a sylgard-coated dish, and the urothelium was removed with the aid of fine forceps, and a dissecting microscope and all tissues were snap-frozen on dry ice prior to processing as previously described (Arms et al. 2010; Arms and Vizzard 2011). The urothelium has suburothelial structures, including the lamina propria, associated with it; the term urothelium in this paper refers to both urothelial and suburothelial structures. To confirm the specificity of our split bladder preparations, urothelium + suburothelium and detrusor samples were examined for the presence of α-smooth muscle actin (1:1,000; Abcam, Cambridge, MA, USA) and uroplakin II (1:25; American Research Products, Belmont, MA, USA) by Western blotting or RT-PCR (Corrow and Vizzard 2007; Cheppudira et al. 2008). In urothelium + suburothelium layers, only uroplakin II was present (data not shown). Conversely, in detrusor samples, only α-smooth muscle actin was present (data not shown). In other instances, the whole urinary bladder was harvested for total RNA extraction.

Real-Time Quantitative Reverse Transcription-Polymerase Chain Reaction

Total RNA was extracted using the STAT-60 total RNA/mRNA isolation reagent (Tel-Test'B', Friendswood, TX, USA) as previously described (Girard et al. 2002; Klinger et al. 2008)). One microgram of RNA per sample was used to synthesize complementary DNA using a mix of random hexamer and oligo dT primers with M-MLV reverse transcriptase (Promega Corp.) in a 25-μl final reaction volume. The quantitative PCR standards for all transcripts were prepared with the amplified cDNA products ligated directly into pCR2.1 TOPO vector using the TOPO TA cloning kit (Invitrogen). The nucleotide sequences of the inserts were verified by automated fluorescent dideoxy dye terminator sequencing (Vermont Cancer Center DNA Analysis Facility). To estimate the relative expression of the receptor transcripts, tenfold serial dilutions of stock plasmids were prepared as quantitative standards. The range of standard concentrations was determined empirically.

Complementary DNA templates, diluted tenfold to minimize the inhibitory effects of the reverse transcription reaction components, were assayed using HotStart-IT SYBR Green qPCR Master Mix (USB, Cleveland, OH, USA) and 300 nM of each primer in a final 25-μl reaction volume. Mouse primers were designed with the upper primer bridging an intron/exon boundary to exclude DNA amplification. TRPV4 and L32 primer sequences have been previously reported (Klinger et al. 2008).

Q-PCR was performed (Applied Biosystems 7500 Fast real-time PCR system, Foster City, CA, USA) using the following standard conditions: (1) serial heating at 94 °C for 2 min; (2) amplification over 45 cycles at 94 °C for 15 s and 55–65 °C for 30 s. The amplified product from these parameters was subjected to SYBR Green I melting analysis by ramping the temperature of the reaction samples from 60 to 95 °C. A single DNA melting profile was observed under these dissociation assay conditions demonstrating amplification of a single unique product free of primer dimers or other anomalous products.

For data analyses, a standard curve was constructed by amplification of serially diluted plasmids containing the target sequence. Data were analyzed at the termination of each assay using sequence detection software (Sequence Detection Software, version 1.3.1; Applied Biosystems, Norwalk, CT, USA). In standard assays, default baseline settings were selected. The increase in SYBR Green I fluorescence intensity (ΔRn) was plotted as a function of cycle number and the threshold cycle was determined by the software as the amplification cycle at which the ΔRn first intersects the established baseline. All data are expressed as the relative quantity of the gene of interest normalized to the relative quantity of the reference gene, L32.

Western Blotting for TRPV4

Whole urinary bladders (n=7–9) were homogenized separately in tissue protein extraction agent (T-PER; Roche, Indianapolis, IN, USA), a mild zwitterionic dialyzable detergent in 25 mM bicine, 150 mM sodium chloride (pH 7.6) containing a protease inhibitor mix (Sigma-Aldrich, St. Louis, MO, USA; 16 μg/ml benzamidine, 2 μg/ml leupeptin, 50 μg/ml lima bean trypsin inhibitor, and 2 μg/ml pepstatin A), and aliquots were removed for protein assay (Merrill et al. 2012b). Lumbosacral DRG were handled as described above with the use of four DRG pooled per level being examined in one sample. Samples (37.5 μg) were suspended in sample buffer for fractionation on gels and subjected to SDS–PAGE. Proteins were transferred to nitrocellulose membranes, and efficiency of transfer was evaluated. Membranes were blocked overnight in a solution of 5 % milk, 3 % bovine serum albumin in Tris-buffered saline with 0.1 % Tween. For immunodetection, the antibodies were used overnight at 4 °C (Table 1). Washed membranes were incubated in species-specific secondary antibodies (Table 1) for 2 h at room temperature for enhanced chemiluminescence detection (Pierce, Rockford, IL, USA). Blots were exposed to Biomax film (Kodak, Rochester, NY, USA) and developed. Blots were analyzed using the Versa Doc 4000 MP Imaging System (BioRad, Hercules, CA). The adjusted volume of each band was analyzed and background intensities subtracted using Quantity One software (BioRad, Hercules, CA; VT Cancer Center DNA Analysis Facility). Images were scanned with an ArtixScan 1800f flatbed scanner (Microtek International,

Table 1 Antibodies, dilutions, and sources

Primary antibody	Manufacturer	Host	Catalog #	Application	Primary antibody dilution	Secondary antibody	Secondary antibody dilution
TRPV4	AbCam (Cambridge, MA, USA)	Rabbit	Ab39260	IHC	1:1,000	Cy2-GAR	1:200
TRPV4	Osenses (Fisher Scientific, Pittsburgh, PA, USA)	Rabbit	OSR00136W	Western blot	1:500	HRP-DAR	1:5,000
PGP9.5	AbD Serotec (Oxford, UK)	Mouse	786-2004	IHC	1:1,000	Cy3-GAM	1:500
Actin	Santa Cruz Biotechnologies (Santa Cruz, CA, USA)	Goat	SC-1616	Western blot	1:1,000	HRP-DAG	1:5,000

Primary and secondary antibodies, sources and dilutions used in immunohistochemical (IHC), and Western blotting approaches

TRPV transient receptor potential vanilloid, *PGP* protein gene product, *Cy* cyanine, *HRP* horseradish peroxidase, *GAR* goat anti-rabbit, *GAM* goat anti-mouse, *DAG* donkey anti-goat, *DAR* donkey anti-rabbit

Carson, CA), the contrast was corrected, the images imported and figures assembled with Adobe Photoshop (San Jose, CA). In this and previous studies (Corrow et al. 2010), we have used actin (Table 1) as a loading control as expression of actin protein was not changed in urinary bladder from NGF-OE mice. Non-specific reactions were assessed by preabsorption treatment with 10^{-6} M of the antigen peptide (blocking peptide for TRPV4, catalog #sc-47527; Santa Cruz Biotechnology, Inc., Santa Cruz, CA USA; Merrill et al. 2012b). Specificity of TRPV4 expression was also confirmed in TRPV4$^{-/-}$ mice (Liedtke and Friedman 2003; Grant et al. 2007).

TRPV4 Immunohistochemistry in Urinary Bladder

Bladder cryosections (10 μm) from female WT and NGF-OE mice (n=7–9) were prepared for immunohistochemistry with an on-slide processing technique (Arms et al. 2010; Arms and Vizzard 2011). For immunohistochemical processing, the cryosections were incubated overnight at room temperature with rabbit anti-TRPV4 (Table 1) diluted in 0.1 M potassium phosphate-buffered saline (KPBS) containing 1 % goat serum. After washing, the preparations were incubated with a Cy3-conjugated species-specific secondary antibody (Table 1) for 2 h at room temperature, rinsed, and mounted with antifade medium (Citifluor, Fisher Scientific) for fluorescent microscopy. In some instances, the bladder was cut open along the midline and pinned to a sylgard-coated dish, and the urothelium was removed with the aid of fine forceps and a dissecting microscope (Arms et al. 2010; Arms and Vizzard 2011). The resulting bladder whole mounts were then used for immunohistochemical detection of TRPV4 as described for bladder cryosections.

Visualization and Semi-quantitative Analysis of TRPV4-IR in the Urinary Bladder

TRPV4 immunoreactivity (IR) in bladder sections was visualized, and images were captured with an Olympus fluorescence photomicroscope. The filter was set with an excitation range of 560–569 nm and an emission range of 610–655 nm for visualization of Cy3. Images were captured, acquired in tagged image file format, and imported into image analysis software (Meta Morph, version 4.5r4, University Imaging, Downingtown, PA) (Arms et al. 2010; Arms and Vizzard 2011). The free hand drawing tool was used to select the urothelium, and the urothelium was measured in total pixels area as previously described (Arms et al. 2010; Arms and Vizzard 2011). A threshold encompassing an intensity range of 100–250 gray-scale values was applied to the region of interest in the least brightly stained condition first. The threshold was adjusted for each experimental series, with concomitantly processed negative controls as a guide for setting background fluorescence. The same threshold was subsequently used for all images. Immunoreactivity was considered to be positive only when the staining for TRPV4 exceeded the established threshold. Percent TRPV4 expression above threshold in the total area selected was calculated. TRPV4-IR in the urothelium was quantified by two individuals in a blinded manner. TRPV4-IR in the urothelium was consistent across all regions (dome, body, neck) of the urinary bladder examined for WT and NGF-OE mice. Semi-quantification of TRPV-IR in the urothelium is presented for the bladder neck region.

Lumbosacral DRG

DRG sections for both WT and NGF-OE mice were processed for TRPV4-immunoreactivity (IR) using an on-slide processing technique (Klinger et al. 2008). Groups (n= 7–9) of littermate WT and NGF-OE were processed simultaneously to decrease the possible incidence of variation in staining and background between tissues and between animals. DRG sections were incubated overnight at room temperature with rabbit anti-TRPV4 (Table 1) in 1 % goat serum and 0.1 M KPBS (phosphate buffer solution with potassium), and then washed (3×15 min) with 0.1 M KPBS, pH 7.4. Tissue was then incubated with a species-specific secondary antibody (Table 1) for 2 h at room

temperature. After several rinses with 0.1 M KPBS, tissues were mounted with Citifluor (Citifluor, London, UK) on slides and coverslipped.

Data Analysis of TRPV4-Labeled DRG

Tissue was examined for visualization of Cy3, and optical sections were acquired using a Zeiss LSM 510 confocal scanning system (Carl Zeiss MicroImaging, Inc., Thornwood, NY) attached to a Zeiss LSM 510 microscope using a plan Fluor 20× and 40× oil objective (Corrow and Vizzard 2009). The filter was set with an excitation range of 560–569 nm and an emission range of 610–655 nm for visualization of Cy3. In DRG from WT and NGF-OE mice, cell profiles exhibiting TRPV4–immunoreactivity (IR) were counted in six to eight sections of each selected DRG (L1, L2, L5–S1). Only cell profiles with a nucleus were quantified. Numbers of TRPV4-immunoreactive cell profiles per DRG section are presented (mean±S.E.M.). The results were not corrected for double counting. Two individuals quantified TRPV4-immunoreactive cells in a blinded fashion. In WT and NGF-OE groups (n=7–9 each), the diameters of DRG cells (35–50 cells) exhibiting cytoplasmic TRPV4-IR were measured long their long and short axes. The average of these two measurements is presented as the mean diameter in micrometers (mean±S.E.M.; Corrow and Vizzard 2009).

Image Capture and Assembly

Digital images were obtained with a charge-coupled device camera (MagnaFire SP; Optronics; Optical Analysis, Nashua, NH) and a LG-3 frame grabber (Scion, Frederick, MD). Exposure times, brightness, and contrast were held constant when acquiring images from experimental or control animals processed and analyzed on the same day. Images were imported into a graphics-editing program (Adobe Photoshop 7.0, Adobe Systems Incorporated, San Jose, CA), assembled, and labeled.

Methodological and Specificity Controls and Assessment of Immunohistochemical Staining in Tissues

Immunohistochemistry and subsequent semi-quantification of TRPV4 expression in tissue sections (urinary bladder, DRG) or whole mount preparations of urinary bladder were performed on WT and NGF-OE tissues simultaneously to reduce the incidence of staining variation that can occur between tissues processed on different days (Corrow and Vizzard 2009). Staining observed in experimental tissue was compared with that observed from experiment-matched negative controls. Urinary bladder sections, whole mounts, and DRG sections exhibiting immunoreactivity that was greater than the background level observed in experiment-matched negative controls were considered positively stained. Control tissues incubated in the absence of primary or secondary antibody were also processed and evaluated for specificity or background staining levels. In the absence of primary antibody, no positive immunostaining was observed. Non-specific reactions were assessed by preabsorption treatment with 10^{-6} M of the antigen peptide [(blocking peptide for TRPV4, Santa Cruz Biotechnology, Inc., (catalog #sc-47527)] (Merrill et al. 2012b). Specificity of TRPV4 expression was also confirmed in TRPV4$^{-/-}$ mice (Liedtke and Friedman 2003; Grant et al. 2007).

Statistical Analyses

Values are expressed as mean±S.E.M. from n mice. Statistical comparisons between groups were made using one-way analysis of variance (ANOVA). Animals, processed and analyzed on the same day, were tested as a block in the ANOVA. Percentage data from image analysis were arcsin transformed to meet the requirements of this statistical test. When F ratios exceeded the critical value ($p \leq 0.05$), the Dunnett's post hoc test was used to compare WT to NGF-OE groups.

Results

NGF Protein and Transcript Expression in Whole Urinary Bladder and Lumbosacral (L1, L2, L5-S1) DRG of Littermate WT and NGF-OE Mice

Consistent with our previous studies (Cheppudira et al. 2008; Schnegelsberg et al. 2010), NGF protein (Fig. 1a) and transcript (data not shown) expression was significantly ($p \leq 0.001$) increased in the urinary bladder of NGF-OE mice. NGF protein (Fig. 1b) and transcript (Fig. 2a) expression was also significantly ($p \leq 0.001$) increased in lumbosacral (L6, S1) DRG of NGF-OE mice. No differences in NGF protein (Fig. 1b) or transcript expression (data not shown) in L5 DRG were observed. Increased NGF protein expression in NGF-OE mice was similar among lumbosacral DRG (L1, L2, L6 and S1) examined. NGF transcript expression in L6-S1 DRG of NGF-OE mice (Fig. 2a) was similar and comparable to NGF transcript expression in L1 and L2 DRG (data not shown).

TRPV4 Transcript Expression in Urothelium + Suburothelium or Detrusor of Littermate WT and NGF-OE Mice

TRPV4 (Fig. 2b) transcript expression was significantly ($p \leq 0.001$) increased in urothelium (Uro) + suburothelium (SU) of NGF-OE mice compared to littermate WT mice, whereas no changes were observed in the detrusor (Fig. 2b). Similarly, TRPV4 transcript expression was significantly ($p \leq 0.001$)

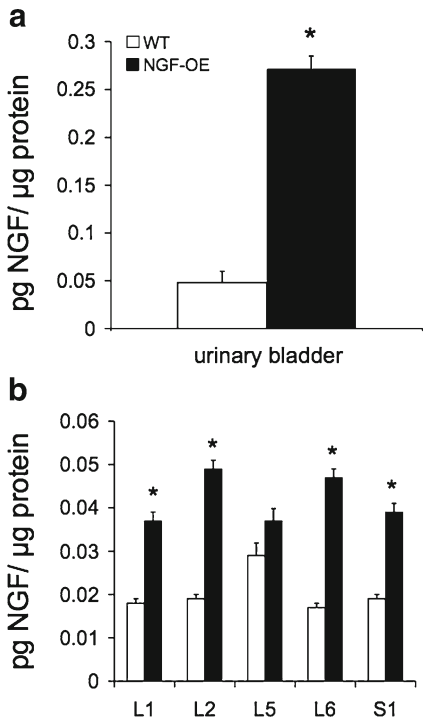

Fig. 1 Increased protein expression of nerve growth factor (NGF) in urinary bladder (**a**) and lumbosacral dorsal root ganglia (DRG) (**b**) in mice with chronic urothelial overexpression of NGF (NGF-OE). NGF protein content was significantly ($p \leq 0.001$) increased in urinary bladder of NGF-OE compared to littermate wild-type (WT) mice (**a**). NGF protein content was significantly ($p \leq 0.001$) increased in lumbosacral (L1, L2, L5-S1) DRG of NGF-OE compared to WT mice (**b**). No change in NGF protein content was observed in L5 DRG of NGF-OE mice compared to WT mice. Increased NGF expression was similar in L1, L2, L6, and S1 DRG from NGF-OE mice. Sample sizes are *n* of 7–9; *$p \leq 0.001$ versus WT

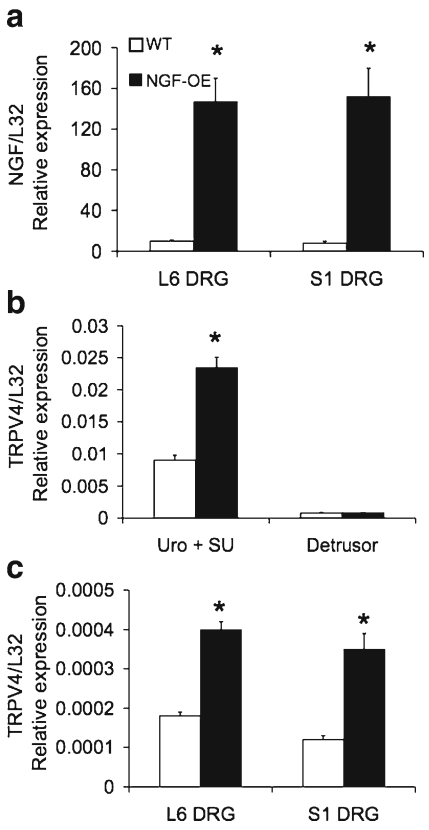

Fig. 2 Regulation of NGF (**a**) and TRPV4 (**b**, **c**) transcript levels in lumbosacral (L6-S1) dorsal root ganglia (DRG; **a**, **c**) and urothelium (Uro) + suburothelium (SU) (**b**) or detrusor smooth muscle (**b**) from wild-type (WT) and nerve growth factor-overexpressing (NGF-OE) mice. NGF transcript expression is significantly ($p \leq 0.001$) increased in L6 and S1 DRG (**a**) of NGF-OE mice. TRPV4 transcript expression is significantly ($p \leq 0.001$) increased in Uro + SU (**b**) and L6-S1 DRG (**c**) of NGF-OE mice compared to littermate WT mice. No change in NGF transcript expression was demonstrated in the detrusor of NGF-OE mice (**b**). Relative expression of NGF (**a**) and TRPV4 (**b**, **c**) transcript expression is normalized to the relative expression of the reference gene, L32. Sample sizes are *n* of 7–9; *$p \leq 0.001$

increased in L6 and S1 DRG of NGF-OE mice (Fig. 2c). The magnitude of increase (2.2–2.6-fold) in TRPV4 transcript expression in L6 and S1 DRG of NGF-OE mice was similar (Fig. 2c).

TRPV4 Protein Expression in Lumbosacral DRG and Uro + SU of Littermate WT and NGF-OE Mice

Western blotting demonstrated significant ($p \leq 0.001$) increases in TRPV4 expression in L6 DRG of NGF-OE mice compared to littermate WT mice (Fig. 3a). Rostral lumbar (L1, L2) and sacral (S1) DRG from NGF-OE mice also exhibited significant increases in TRPV4 expression compared to WT mice (data not shown). Little, if any, TRPV4 expression was evident in L6 DRG harvested from TRPV4$^{-/-}$ mice (Fig. 3a). Western blotting demonstrated significant ($p \leq 0.001$) increases in TRPV4 expression in Uro + SU in NGF-OE mice compared to littermate WT mice (Fig. 3b). Little, if any, TRPV4 expression was present in Uro + SU harvested from TRPV4$^{-/-}$ mice (Fig. 3b).

Urothelial TRPV4-IR in Littermate WT and NGF-OE Mice

Faint TRPV4-IR was present in the urothelium of cryostat bladder sections of WT mice (Fig. 4a, c); however, TRPV4-IR was more intense in urothelium of NGF-OE mice (Fig. 4b, d, f). Semi-quantitative analyses revealed significant ($p \leq 0.001$) increases in TRPV4-IR in the urothelium of NGF-OE mice (Fig. 4e). No regional differences in TRPV4-IR in the urothelium of the dome, body or neck regions of the urinary bladder were observed in WT or NGF-OE mice. TRPV4-IR was observed in all cell layers (apical, intermediate, and basal) of the urothelium of WT and NGF-OE mice

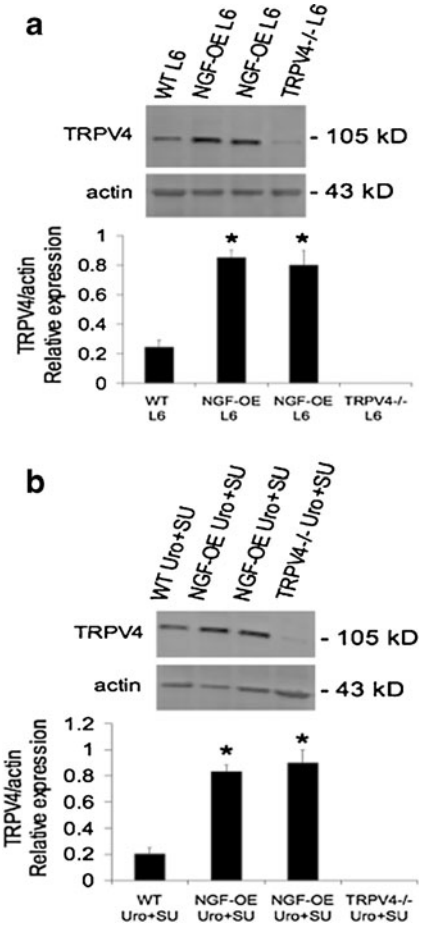

Fig. 3 Western blot analyses of TRPV4 expression in lumbar (L) 6 dorsal root ganglia (DRG) (**a**) and urothelium (Uro) + suburothelium (SU) from wild-type (WT), NGF-overexpressing (OE) and TRPV4$^{-/-}$ mice. Representative Western blot of TRPV4 protein expression in L6 DRG from WT, NGF-OE, and TRPV4$^{-/-}$ mice (**a**). Summary histogram of the relative expression of TRPV4 protein normalized to actin expression in L6 DRG from WT, NGF-OE, and TRPV4$^{-/-}$ mice (**a**). Representative Western blot of TRPV4 protein expression in Uro + SU from WT, NGF-OE, and TRPV4$^{-/-}$ mice (**b**). Summary histogram of the relative expression of TRPV4 protein normalized to actin expression in Uro + SU from WT, NGF-OE, and TRPV4−/− mice (**b**). Sample sizes are n of 7–9; *$p \leq 0.001$ versus WT

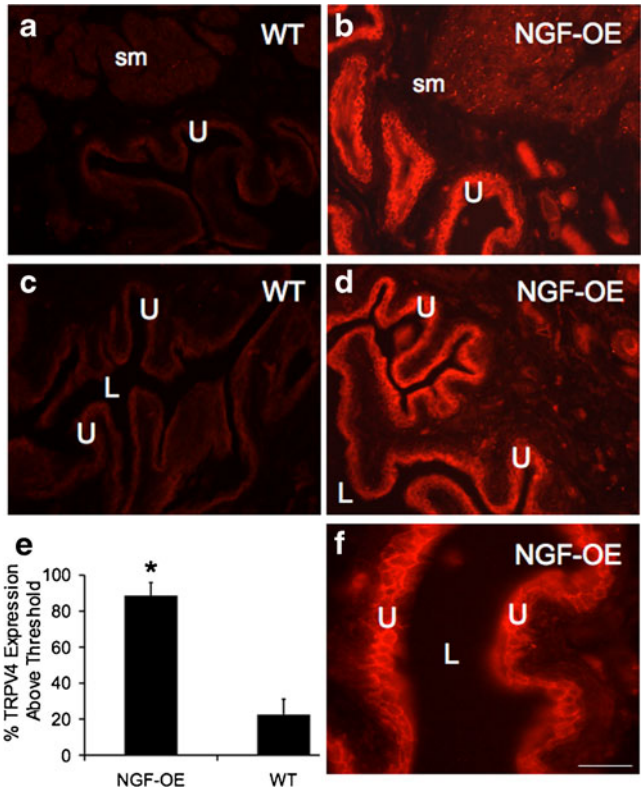

Fig. 4 TRPV4-immunoreactivity (*IR*) in cryostat sections of urinary bladder from WT and NGF-OE mice. In WT mice, faint TRPV4-IR was present in urothelium (*U*) and detrusor smooth muscle (*sm*) (**a**, **c**). Chronic overexpression of NGF in the U increased TRPV4-IR in U (**b**, **d**, **f**) and detrusor sm (**b**). Higher power fluorescence image of TRPV4-IR in U (**f**). TRPV4-IR was exhibited in all cellular layers of the U (**a**–**d**, **f**) in WT and NGF-OE mice. TRPV4-IR was present in the U throughout the bladder dome, body, and neck regions. For all images, exposure times were held constant, and all tissues were processed simultaneously. **e** Histogram of TRPV4 expression above threshold in the U of NGF-OE and WT mice expressed as a percentage of control. **e** TRPV4-IR above threshold in U was significantly ($p \leq 0.001$) increased in NGF-OE mice. Calibration *bar* represents 50 μm in **a**–**d** and 25 μm in **f**. Data are a summary of n=7–9 for each group. *L* lumen

(Fig. 4b, d, f). Although not a focus of this study, TRPV4-IR was also expressed in the detrusor of both WT and NGF-OE mice and increased in detrusor of NGF-OE mice (Fig. 4b). However, no change in TRPV4 mRNA in detrusor of NGF-OE mice was demonstrated (Fig. 2b). TRPV4-IR was largely absent from the lamina propria of WT and NGF-OE mice (Fig. 4a–d, f).

TRPV4-IR in Suburothelial Plexus of WT and NGF-OE Mice

In whole mount preparations, TRPV4-IR was observed in the suburothelial nerve plexus throughout the entire urinary bladder of WT and NGF-OE mice (Fig. 5a–d). Chronic urothelial NGF-OE increased the appearance of TRPV4-IR in the suburothelial plexus (Fig. 5a, c, d). The density of the TRPV4-IR in suburothelial nerve fibers was greatest in the neck region in WT and NGF-OE mice, and our semi-quantitative analysis of TRPV4-IR was restricted to the suburothelial plexus in this region. A significant ($p \leq 0.001$) increase in the density of the TRPV4-IR nerve fibers in the bladder neck region was observed in NGF-OE mice (Fig. 5e). Fine and thicker caliber TRPV4-immunoreactive neuronal fibers were observed in the suburothelial plexus in both WT and NGF-OE mice (Fig. 5a–d). TRPV4-IR in the suburothelial nerve plexus also exhibited immunoreactivity for the pan neuronal marker, protein gene product 9.5

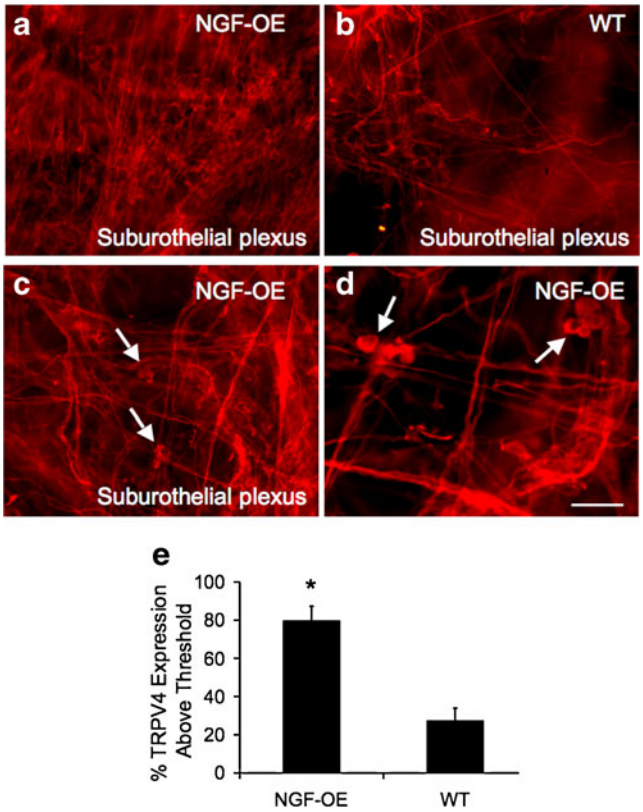

Fig. 5 Fluorescence photographs of TRPV4-immunoreactivity (IR) in the suburothelial plexus in the bladder neck region in whole mount preparations of the urinary bladder from WT and NGF-OE mice. Dense TRPV4-IR was present in the suburothelial plexus in the bladder neck region of NGF-OE mice (**a**) compared to WT mice with less dense TRPV-IR in the suburothelial plexus (**b**). In NGF-OE mice, small clusters of TRPV4-IR cells were located within the suburothelial plexus of NGF-OE mice (**c**, *arrows*). Higher power immunofluorescence images of TRPV4-IR in the suburothelial plexus and in clusters of cells (**d**, *arrows*) within the suburothelial plexus in NGF-OE mice. WT mice did not exhibit clusters of TRPV4-IR cells in the suburothelial plexus. **e** TRPV4-IR above threshold in the suburothelial plexus was significantly ($p \leq 0.001$) increased in NGF-OE mice. Calibration *bar* represents 50 μm in **a**, **b** and 25 μm in **c**, **d**. Data are a summary of $n=7–9$ for each group

(data not shown). In whole mount preparations of the suburothelial plexus from NGF-OE mice, small clusters of TRPV4-IR cells (5–7) were observed in the plexus (Fig. 5c, d). Within the suburothelial plexus of NGF-OE mice, 10–12 clusters were commonly observed. No TRPV4-IR cell clusters were observed in the suburothelial plexus of WT mice.

TRPV4-IR in Suburothelial Plexus and Urothelium in Whole Mount Preparations of Urinary Bladder of NGF-OE Mice

Consistent with TRPV4-IR in the urothelium of cryostat bladder sections from WT and NGF-OE mice, whole mount preparations of the urothelium also revealed

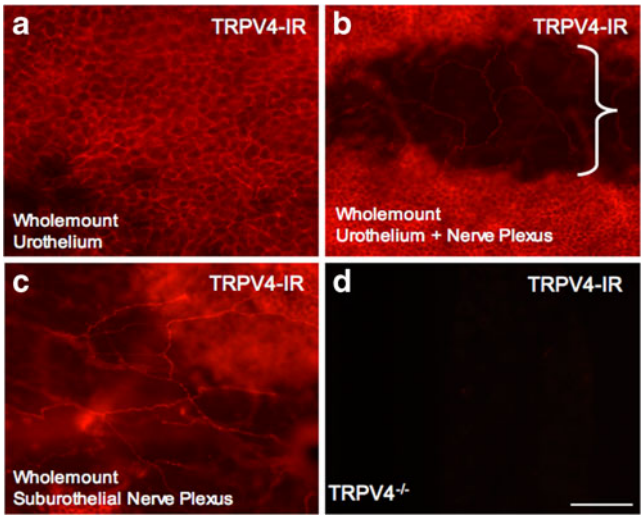

Fig. 6 TRPV4-immunoreactivity (IR) in whole mount preparations of the urinary bladder from NGF-OE mice. In whole mount preparations, robust TRPV4-IR was present throughout the urothelium in the bladder dome, body, and neck regions (**a**, **b**). With the urothelium dissected, TRPV4-IR is observed in the suburothelial nerve plexus (**b**, *bracketed region*). The *bracketed region* (**b**) is an area with the urothelium removed showing the suburothelial nerve plexus as in **c**. TRPV4-IR was present in the suburothelial plexus (**c**) in the bladder dome, body, and neck and with greatest density of TRPV4-immunoreactive nerve fibers being present in the bladder neck. The specificity of the TRPV4 antibody used was verified in urinary bladder harvested from TRPV4$^{-/-}$ mice that did not exhibit TRPV4-IR (**d**). Calibration *bar* represents 50 μm in **a**–**d**

extensive TRPV4-IR throughout the urothelium of NGF-OE mice (Fig. 6a). When the urothelium was removed, TRPV4-IR nerve fibers in the suburothelial plexus could also be observed in whole mount preparations (Fig. 6b, c) of NGF-OE mice. Tissues (e.g., urinary bladder, DRG) from TRPV4$^{-/-}$ mice did not exhibit TRPV4-IR (Fig. 6d).

Numbers of TRPV4-Immunoreactive Lumbosacral DRG Cells Are Increased in NGF-OE Compared to Littermate WT Mice

Lumbosacral (L1, L2, L5-S1) DRG cells exhibited positive cytoplasmic staining for TRPV4-IR in littermate WT and NGF-OE mice (Fig. 7a–d). TRPV4-IR nerve fibers were also observed throughout the lumbosacral DRG in both WT and NGF-OE mice (Fig. 7a–d). In NGF-OE mice, significantly ($p \leq 0.001$) greater numbers of TRPV4-IR cells were observed in the L1, L2, L6 and S1 DRG (Fig. 7b–d) consistent with Western blotting studies (Fig. 3). Among lumbosacral DRG from NGF-OE mice, the numbers of TRPV4-immunoreactive cells were significantly ($p \leq 0.01$) greater in rostral lumbar (L1, L2 DRG) compared to caudal lumbosacral (L6, S1) DRG. No differences in numbers of TRPV4-immunoreactive cells in L5 DRG were observed

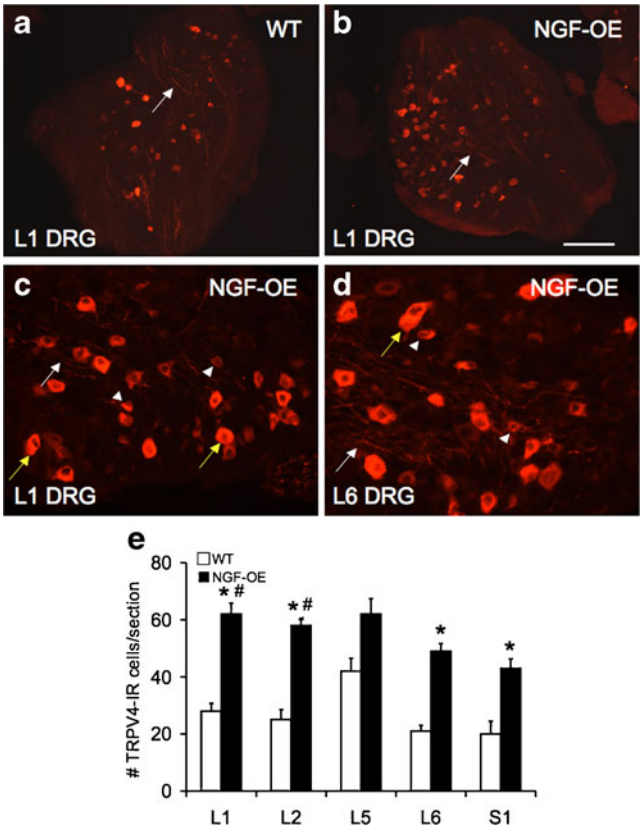

Fig. 7 TRPV4-IR in lumbosacral dorsal root ganglia in WT and NGF-OE mice. Lower power immunofluorescence images of TRPV4-IR in L1 DRG from WT (**a**) and NGF-OE mice (**b**). Higher power images of TRPV4-IR in L1 (**c**) and L6 (**d**) DRG from NGF-OE mice. TRPV4-IR nerve fibers were present throughout DRG in WT and NGF-OE mice (**a**–**d**, *white arrows*). TRPV4-IR was present in both small (**c**, **d**, *arrowheads*) and larger (**c**, **d**, *yellow arrows*) DRG cells. **e** Summary histogram of the number of TRPV4-IR cells per section in L1, L2, L5-S1 DRG in WT and NGF-OE mice. Numbers of TRPV4-IR DRG cells were significantly ($*p \leq 0.001$) increased in L1, L2, L6, and S1 DRG from NGF-OE mice compared to WT. No changes in TRPV4-IR were observed in L5 DRG between NGF-OE and WT mice. Numbers of TRPV4-IR DRG cells were significantly ($^{\#}p \leq 0.01$) greater in L1 and L2 DRG compared to L6 and S1 DRG in NGF-OE mice. Calibration *bar* represents 80 μm in **a**, **b**; 25 μm in **c**, **d**. Data are a summary of $n=7$–9 for each group

between WT and NGF-OE mice (Fig. 7e). TRPV4-IR was observed primarily in small diameter DRG cells (16.8±2.4 μm), but some larger DRG cells (23.3±2.6 μm) also exhibited TRPV4-IR in WT mice. In NGF-OE mice, TRPV4-IR was also observed in small (21.3±2.2 μm) and larger (26.2±2.7 μm) diameter DRG cells (Fig. 7c, d).

Discussion

The current studies address the target tissue dependence of TRPV4 expression in the urinary bladder and lumbosacral DRG using a recently characterized transgenic mouse model with chronic overexpression of nerve growth factor (NGF-OE) in the urothelium (Schnegelsberg et al. 2010). TRPV4 transcript and protein expression was significantly ($p \leq 0.001$) increased in the urothelium + suburothelium and suburothelial nerve plexus of the urinary bladder and in small- and medium-sized lumbosacral (L1, L2, L6-S1) DRG cells from NGF-OE mice compared to littermate WT mice. NGF-OE mice exhibit significant ($p \leq 0.001$) increases in NGF transcript and protein in the urothelium + suburothelium and lumbosacral DRG. As previously demonstrated, NGF-OE mice exhibit increased urinary frequency, hyperinnervation of the urinary bladder, and increased pelvic sensitivity (Schnegelsberg et al. 2010). In addition to overexpression of NGF in the urothelium, a number of pleiotropic changes in other growth factor/receptor and neuropeptide/receptor systems have been demonstrated (Cheppudira et al. 2008; Schnegelsberg et al. 2010; Girard et al. 2011, 2012). Ongoing studies are characterizing the functional roles of TRPV4 expression in the sensory limb (DRG, urothelium) of the micturition reflex in WT and NGF-OE mice. Previous studies have demonstrated that TRPV4 blockade reduces voiding frequency and TRPV4$^{-/-}$ mice exhibit a decrease in voiding frequency and an increase in bladder capacity and void volume (Gevaert et al. 2007). It remains to be determined if TRPV4 blockade in NGF-OE mice reduces voiding frequency and pelvic sensitivity (Schnegelsberg et al. 2010).

There are more than 50 TRP channels described in diverse species from yeast to human and 28 known mammalian TRP channels in 7 subfamilies: TRPC (canonical), TRPM (melastatin), TRPV (vanilloid), TRPA (ankyrin), TRPP (polycystin), TRPML (mucolipin), and TRPN (no mechanopotential; Everaerts et al. 2008). Studies indicate that several TRP channels, including members of the vanilloid (TRPV1, TRPV2, TRPV4), melastatin (TRPM8), and ankyrin (TRPA1) families, are expressed in the urinary bladder and may act as sensory transducers of stretch and/or chemical irritation in the lower urinary tract (Andersson et al. 2010). Most of these TRP channels are also implicated in bladder diseases such as overactive bladder (OAB) and painful bladder syndrome (Nilius et al. 2007; Everaerts et al. 2008). Therefore, it is important to understand the expression as well as the mechanisms by which these channels act in order to create potential therapeutic targets for these diseases. TRPV1 and TRPV4 are the most widely studied TRP channels pertaining to their role in the urinary bladder (Andersson et al. 2010). TRPV4 expression has been demonstrated in basal and intermediate urothelial cells of mice and rats (Birder et al. 2007; Gevaert et al. 2007; Kullmann et al. 2009; Mochizuki et al. 2009; Yamada et al. 2009).

TRPV4 is also expressed in the detrusor muscle, but urothelial TRPV4 expression is approximately 20–36-fold greater (Thorneloe et al. 2008; Xu et al. 2009) compared to detrusor. In addition, TRPV4 expression has been demonstrated in DRG neurons (Suzuki et al. 2003b) innervating viscera and has been implicated in neurogenic inflammation (Vergnolle et al. 2010). An abnormal urine voiding pattern has been reported in the TRPV4$^{-/-}$ mice (Angelico and Testa 2010), characterized by a decrease in voiding frequency and an increase in bladder capacity and void volume (Thorneloe et al. 2008; Everaerts et al. 2010). TRPV4 channel agonists increase bladder hyperactivity, whereas TRPV4 antagonists result in a decrease in bladder activity, making it a promising target for OAB and other bladder disorders (Araki 2011; Olsen et al. 2011). In addition, TRPV4$^{-/-}$ mice have a decreased sensitivity to tail pressure, show deficits in mechanically evoked paw withdrawal responses (Liedtke and Friedman 2003; Suzuki et al. 2003b). Recent studies from our laboratory using a cyclophosphamide-induced cystitis rodent model (Merrill et al. 2012b) and a repeated variate stress rodent model (Merrill et al. 2012a) have demonstrated increased TRPV4 expression in the urinary bladder and blockade of TRPV4 with HC067047 reduced voiding frequency.

Increased urinary bladder NGF content may underlie many of the sensory changes that occur in patients with OAB symptoms or BPS/IC, including irritative voiding symptoms and pain in the case of BPS/IC (Kim et al. 2005, 2006). Altered NGF content is associated with urinary bladder inflammation and dysfunction in rodents (Vizzard 2001; Zvarova et al. 2004; Braas et al. 2006; Klinger and Vizzard 2008). BPS/IC is one type of chronic pain syndrome characterized by pain, pressure, or discomfort perceived to be bladder related with at least one urinary symptom (Hanno et al. 2010). Pain and altered bladder/visceral hypersensitivity in BPS/IC patients may involve organizational or functional changes in peripheral bladder afferents and central pathways such that bladder afferent neurons become sensitized and hyperresponsive to normally innocuous stimuli such as bladder filling (Driscoll and Teichman 2001). Our previous studies (Schnegelsberg et al. 2010) revealed that urothelium-specific overexpression of NGF in the urinary bladder of transgenic mice (1) stimulates neuronal sprouting or proliferation in the urinary bladder; (2) produces local inflammatory changes in the urinary bladder; (3) produces urinary bladder hyperreflexia; and (4) results in increased referred somatic hypersensitivity. Elevated levels of neurotrophins have also been detected in the urine of women (Okragly et al. 1999) and in the urothelium of individuals with BPS/IC or other painful bladder conditions (Lowe et al. 1997). More recently, it was demonstrated that urinary NGF levels are increased in patients with OAB symptoms associated with detrusor overactivity, stress urinary incontinence, or bladder outlet obstruction (Okragly et al. 1999; Kim et al. 2005, 2006; Liu and Kuo 2007; Liu et al. 2008; Liu and Kuo 2008; Yokoyama et al. 2008).

Additional NGF-mediated changes might contribute to the urinary bladder hyperreflexia and pelvic hypersensitivity observed in these mice (Schnegelsberg et al. 2010), such as stimulation/recruitment of bladder mast cells, modulation of local neuroinflammatory responses, upregulation of neuropeptide/receptor systems and neurotrophin/receptor systems and ion channels in the urinary bladder, including TRP channels (Cheppudira et al. 2008; Schnegelsberg et al. 2010; Girard et al. 2011, 2012). Our demonstration that TRPV4 transcript and protein expression are increased in the urothelium and suburothelium and lumbosacral DRG of NGF-OE mice is consistent with previous studies demonstrating that TRPV1 and TRPA1 function and modulation in sensory neurons are dependent upon target tissue expression of NGF and GDNF (Malin et al. 2011). In addition, previous studies demonstrate that early neonatal colon injury results in a long-lasting visceral hypersensitivity, possibly driven by an early increase in growth factor expression and long-term changes in TRPA1 function (Christianson et al. 2010). Ongoing studies are determining effects of TRPV4 antagonism on altered micturition reflex function in the NGF-OE mouse model.

Numerous studies have demonstrated TRPV4 expression in the urinary bladder (e.g., urothelium and detrusor), and functional roles for TRPV4 expression have resulted from pharmacological studies and studies involving TRPV4 null mice (Gevaert et al. 2007; Nilius et al. 2007; Everaerts et al. 2008, 2010; Thorneloe et al. 2008; Andersson et al. 2010; Araki 2011; Eid 2011). Numerous studies have described the expression and distribution of TRPV4 in the urothelium (freshly isolated and cultured) of diverse species including mouse, rat, guinea pig, and human (Everaerts et al. 2008; Kullmann et al. 2009; Xu et al. 2009; Everaerts et al. 2010; Janssen et al. 2011). Our studies confirm TRPV4 transcript and protein expression in apical, basal, and intermediate urothelial cells in mice and extend these findings by demonstrating increased TRPV4 expression in the urothelium + suburothelium in mice with chronic overexpression of NGF (NGF-OE) in the urothelium. Recent morphological studies in human bladder urothelium have localized TRPV4 to adherence junctions consistent with the suggestion that TRPV4 is activated by bladder stretch (Janssen et al. 2011). The function of TRPV4 was originally hypothesized to be as a sensory (mechanosensor, osmosensor; Voets et al. 2005) transducer, and more recent studies have expanded TRPV4 functions to include sensing mechanical pressure, osmolality, and warmth (Liedtke and Friedman 2003; Suzuki et al. 2003a). Consistent with these roles, bladder strips from TRPV4 null mice exhibit reduced contraction amplitude and decreased stretch-evoked ATP release in

isolated whole bladder (Gevaert et al. 2007). In addition, mechanical stretch of urothelial cells activates TRPV4 resulting in increased $[Ca^{2+}]_i$ and ATP release (Birder et al. 2007; Mochizuki et al. 2009). It has been suggested that the TRPV4 channel participates in the mechanosensory pathway in the urinary bladder and that mechanical activation of TRPV4 in urothelial cells results in ATP release and signaling in the micturition reflex pathway (Christensen and Corey 2007).

TRPV4 expression has been demonstrated in DRG neurons (Suzuki et al. 2003b; Yamada et al. 2009), and this study confirms TRPV4 expression in lumbosacral DRG and also demonstrates increased TRPV4 transcript and protein expression in lumbosacral DRG from NGF-OE mice. Roles for TRPV4 in afferent nerves have been suggested to include contributions to neurogenic inflammation, nociceptor sensitization and associated mechanical allodynia, mechanical hyperalgesia, and thermal hyperalgesia (Andersson et al. 2010; Araki et al. 2010). In addition to demonstrating increased TRPV4 expression in DRG from NGF-OE mice, the present study also demonstrated TRPV4 expression in the suburothelial nerve plexus both in WT and NGF-OE mice with NGF-OE mice exhibiting increased density of TRPV4-immunoreactive nerves in the suburothelial plexus. Although we did not label bladder afferent cells in the lumbosacral DRG with conventional dye-tracing techniques, the extensive TRPV4-IR in the suburothelial nerve plexus is highly indicative that TRPV4-IR in the DRG represents some bladder afferent cells. It has been suggested that TRPV4 participates in mechanosensory activation of urothelial cells and subsequent release of ATP (Christensen and Corey 2007). It has also been suggested that TRPV4 expression in sensory neurons (Suzuki et al. 2003b; Yamada et al. 2009) and now demonstrated in bladder afferent terminals in the suburothelial nerve plexus raises the possibility that TRPV4 channels on bladder afferent terminals may be directly mechanically gated by urinary bladder distention (Andersson et al. 2010). Such a mechanism of TRPV4 activation by bladder distention on bladder afferent terminals may be independent of TRPV4 activation of urothelial cells (Andersson et al. 2010). Future studies are necessary to determine if TRPV4 activation on bladder afferent terminals is direct (mechanically gated) and/or indirect via TRPV4 activation of urothelial cells, release of ATP, and activation of purinergic receptors on bladder afferent terminals. In our previous studies, we described small clusters of cells embedded in the suburothelial nerve plexus of NGF-OE mice that exhibit neuropeptide (CGRP, substance P) immunoreactivity (Schnegelsberg et al. 2010). In the current study, small clusters of TRPV4-IR cells embedded in the suburothelial nerve plexus of NGF-OE mice were also observed. Previous studies have described co-localization of TRPV4 and neuropeptides in DRG neurons of several species (Vergnolle et al. 2010). The functional significance of these peptidergic- and TRPV4-immunoreactive cells is unknown, but similar cells are present during early postnatal development of the urinary bladder in diverse species (Zvarova and Vizzard 2005), and although the function of such cells is unknown, they do demonstrate the complexity of the peripheral innervation of the urinary bladder.

Conclusions

In a transgenic mouse model with chronic overexpression of NGF in the urothelium, we demonstrate NGF regulation of TRPV4 expression (transcript, protein) in the sensory limb of the micturition reflex including the urothelium, lumbosacral DRG neurons, and peripheral bladder afferent terminals in the suburothelial nerve plexus. Future studies will address the functional contributions of TRPV4 to increased voiding frequency and somatic sensitivity in the NGF-OE mouse model (Schnegelsberg et al. 2010) and will address the potential significance of targeting TRPV4 to improve urinary bladder function.

Acknowledgments The authors thank Dr. Debra Cockayne, Roche Palo Alto for the generous gift of NGF-OE mouse breeders. The authors thank Dr. Andy Grant, King's College, London and Dr. Wolfgang Liedtke, Duke University Medical Center, Durham, NC for the generous gift of $TRPV4^{-/-}$ tissues and $TRPV4^{-/-}$ mouse breeders. The authors gratefully acknowledge the technical expertise and support provided by the VT Cancer Center DNA Analysis Facility.

Grants This work was funded by National Institutes of Health (NIH) grants DK051369 (MAV), DK060481 (MAV), and DK065989 (MAV). This publication was also supported by grants from the National Center for Research Resources (5 P30 RR 032135) and the National Institute of General Medical Sciences (8 P30 GM 103498) from the NIH. Ms. Cristina Robinson was a part of the 2012 summer neuroscience undergraduate research fellow (SNURF) program supported, in part, through a Center of Biomedical Research Excellence (COBRE) in Neuroscience funded by the National Center for Research Resources of the NIH.

References

Andersson KE, Gratzke C, Hedlund P (2010) The role of the transient receptor potential (TRP) superfamily of cation-selective channels in the management of the overactive bladder. BJU Int 106:1114–1127

Angelico P, Testa R (2010) TRPV4 as a target for bladder overactivity. F1000 Biol Rep 2

Araki I (2011) TRP channels in urinary bladder mechanosensation. Adv Exp Med Biol 704:861–879

Araki I, Yoshiyama M, Kobayashi H, Mochizuki T, Du S, Okada Y, Takeda M (2010) Emerging families of ion channels involved in urinary bladder nociception. Pharmaceuticals 3:2248–2267

Arms L, Vizzard MA (2011) Role for pAKT in rat urinary bladder with cyclophosphamide (CYP)-induced cystitis. Am J Physiol Renal Physiol 301:F252–F262

Arms L, Girard BM, Vizzard MA (2010) Expression and function of CXCL12/CXCR4 in rat urinary bladder with cyclophosphamide-induced cystitis. Am J Physiol Renal Physiol 298:F589–F600

Berry SH, Elliott MN, Suttorp M et al (2011) Prevalence of symptoms of bladder pain syndrome/interstitial cystitis among adult females in the United States. J Urol 186:540–544

Birder L, Kullmann FA, Lee H, Barrick S, de Groat W, Kanai A, Caterina M (2007) Activation of urothelial transient receptor potential vanilloid 4 by 4alpha-phorbol 12,13-didecanoate contributes to altered bladder reflexes in the rat. J Pharmacol Exp Ther 323:227–235

Braas KM, May V, Zvara P et al (2006) Role for pituitary adenylate cyclase activating polypeptide in cystitis-induced plasticity of micturition reflexes. Am J Physiol Regul Integr Comp Physiol 290:R951–R962

Cheppudira BP, Girard BM, Malley SE, Schutz KC, May V, Vizzard MA (2008) Upregulation of vascular endothelial growth factor isoform VEGF-164 and receptors (VEGFR-2, Npn-1, and Npn-2) in rats with cyclophosphamide-induced cystitis. Am J Physiol Renal Physiol 295:F826–F836

Christensen AP, Corey DP (2007) TRP channels in mechanosensation: direct or indirect activation? Nat Rev Neurosci 8:510–521

Christianson JA, Bielefeldt K, Malin SA, Davis BM (2010) Neonatal colon insult alters growth factor expression and TRPA1 responses in adult mice. Pain 151:540–549

Clemons JL, Arya LA, Myers DL (2002) Diagnosing interstitial cystitis in women with chronic pelvic pain. Obstet Gynecol 100:337–341

Corrow KA, Vizzard MA (2007) Phosphorylation of extracellular signal-regulated kinases in urinary bladder in rats with cyclophosphamide-induced cystitis. Am J Physiol Regul Integr Comp Physiol 293:R125–R134

Corrow KA, Vizzard MA (2009) Phosphorylation of extracellular signal-regulated kinases in bladder afferent pathways with cyclophosphamide-induced cystitis. Neuroscience 163:1353–1362

Corrow K, Girard BM, Vizzard MA (2010) Expression and response of acid-sensing ion channels in urinary bladder to cyclophosphamide-induced cystitis. Am J Physiol Renal Physiol 298:F1130–F1139

Dinarello CAD (1997) Proinflammatory and anti-inflammatory cytokines as mediators in the pathogenesis of septic shock. Chest 112:321S–329S

Dray A (1995) Inflammatory mediators of pain. Br J Anaesth 75:125–131

Driscoll A, Teichman JMH (2001) How do patients with interstitial cystitis present? J Urol 166:2118–2120

Eid SR (2011) Therapeutic targeting of TRP channels—the TR(i)P to pain relief. Curr Top Med Chem 11:2118–2130

Evans RJ, Moldwin RM, Cossons N, Darekar A, Mills IW, Scholfield D (2011) Proof of concept trial of tanezumab for the treatment of symptoms associated with interstitial cystitis. J Urol 185:1716–1721

Everaerts W, Gevaert T, Nilius B, De Ridder D (2008) On the origin of bladder sensing: Tr(i)ps in urology. Neurourol Urodyn 27:264–273

Everaerts W, Zhen X, Ghosh D et al (2010) Inhibition of the cation channel TRPV4 improves bladder function in mice and rats with cyclophosphamide-induced cystitis. Proc Natl Acad Sci U S A 107:19084–19089

Gevaert T, Vriens J, Segal A et al (2007) Deletion of the transient receptor potential cation channel TRPV4 impairs murine bladder voiding. J Clin Invest 117:3453–3462

Girard BM, May V, Bora SH, Fina F, Braas KM (2002) Regulation of neurotrophic peptide expression in sympathetic neurons: quantitative analysis using radioimmunoassay and real-time quantitative polymerase chain reaction. Regul Pept 109:89–101

Girard BM, Malley SE, Vizzard MA (2011) Neurotrophin/receptor expression in urinary bladder of mice with overexpression of NGF in urothelium. Am J Physiol Renal Physiol 300:F345–F355

Girard BM, Tompkins JD, Parsons RL, May V, Vizzard MA (2012) Effects of CYP-induced cystitis on PACAP/VIP and receptor expression in micturition pathways and bladder function in mice with overexpression of NGF in urothelium. J Mol Neurosci 48(3):730–743

Grant AD, Cottrell GS, Amadesi S et al (2007) Protease-activated receptor 2 sensitizes the transient receptor potential vanilloid 4 ion channel to cause mechanical hyperalgesia in mice. J Physiol 578:715–733

Hanno P, Lin A, Nordling J, Nyberg L, van Ophoven A, Ueda T, Wein A (2010) Bladder pain syndrome committee of the international consultation on incontinence. Neurourol Urodyn 29:191–198

Ho N, Koziol JA, Parsons CL (1997) Epidemiology of interstitial cystitis. In: Sant GR (ed) Interstitial cystitis. Lippincott-Raven Publishers, Philadelphia, pp 9–16

Janssen DA, Hoenderop JG, Jansen KC, Kemp AW, Heesakkers JP, Schalken JA (2011) The mechanoreceptor TRPV4 is localized in adherence junctions of the human bladder urothelium: a morphological study. J Urol 186:1121–1127

Johansson SL, Ogawa K, Fall M (1997) The pathology of interstitial cystitis. In: Sant GR (ed) Interstitial cystitis. Lippincott-Raven Publishers, Philadelphia, pp 143–152

Kim JC, Park EY, Hong SH, Seo SI, Park YH, Hwang TK (2005) Changes of urinary nerve growth factor and prostaglandins in male patients with overactive bladder symptom. Int J Urol 12:875–880

Kim JC, Park EY, Seo SI, Park YH, Hwang TK (2006) Nerve growth factor and prostaglandins in the urine of female patients with overactive bladder. J Urol 175:1773–1776, discussion 1776

Klinger MB, Vizzard MA (2008) Role of p75NTR in female rat urinary bladder with cyclophosphamide-induced cystitis. Am J Physiol Renal Physiol 295:F1778–F1789

Klinger MB, Girard B, Vizzard MA (2008) p75(NTR) expression in rat urinary bladder sensory neurons and spinal cord with cyclophosphamide-induced cystitis. J Comp Neurol 507:1379–1392

Kullmann FA, Shah MA, Birder LA, de Groat WC (2009) Functional TRP and ASIC-like channels in cultured urothelial cells from the rat. Am J Physiol Renal Physiol 296:F892–F901

Liedtke W, Friedman JM (2003) Abnormal osmotic regulation in trpv4 −/− mice. Proc Natl Acad Sci U S A 100:13698–13703

Lindsay RM, Harmar AJ (1989) Nerve growth factor regulates expression of neuropeptide genes in adult sensory neurons. Nature 337:362–367

Liu HT, Kuo HC (2007) Intravesical botulinum toxin A injections plus hydrodistension can reduce nerve growth factor production and control bladder pain in interstitial cystitis. Urology 70:463–468

Liu HT, Kuo HC (2008) Urinary nerve growth factor levels are increased in patients with bladder outlet obstruction with overactive bladder symptoms and reduced after successful medical treatment. Urology 72:104–108

Liu HT, Chancellor MB, Kuo HC (2008) Urinary nerve growth factor level could be a biomarker in the differential diagnosis of mixed urinary incontinence in women. BJU Int 102(10):1440–1444

Lowe EM, Anand P, Terenghi G, Williams-Chestnut RE, Sinicropi DV, Osborne JL (1997) Increased nerve growth factor levels in the urinary bladder of women with idiopathic sensory urgency and interstitial cystitis. Br J Urol 79:572–577

Malin S, Molliver D, Christianson JA, Schwartz ES, Cornuet P, Albers KM, Davis BM (2011) TRPV1 and TRPA1 function and modulation are target tissue dependent. J Neurosci 31:10516–10528

Merrill L, Girard B, Peterson A, Vizzard MA (2012a) Role of vanilloid transient receptor potential cation channel (TRPV) 4 in bladder dysfunction in response to repeated variate stress (RVS) in male rats. 2012 Neurosci. Meeting Planner Program No. 484.13

Merrill L, Girard BM, May V, Vizzard MA (2012b) Transcriptional and translational plasticity in rodent urinary bladder TRP channels

with urinary bladder inflammation, bladder dysfunction, or postnatal maturation. J Mol Neurosci 48:744–756

Mochizuki T, Sokabe T, Araki I et al (2009) The TRPV4 cation channel mediates stretch-evoked Ca2+ influx and ATP release in primary urothelial cell cultures. J Biol Chem 284:21257–21264

Moran MM, McAlexander MA, Biro T, Szallasi A (2011) Transient receptor potential channels as therapeutic targets. Nat Rev Drug Discov 10:601–620

Nilius B, Owsianik G, Voets T, Peters JA (2007) Transient receptor potential cation channels in disease. Physiol Rev 87:165–217

Okragly AJ, Niles AL, Saban R et al (1999) Elevated tryptase, nerve growth factor, neurotrophin-3 and glial cell line-derived neurotrophic factor levels in the urine of interstitial cystitis and bladder cancer patients. J Urol 161:438–442

Olsen SM, Stover JD, Nagatomi J (2011) Examining the role of mechanosensitive ion channels in pressure mechanotransduction in rat bladder urothelial cells. Ann Biomed Eng 39:688–697

Petrone RL, Agha AH, Roy JB, Hurst RE (1995) Urodynamic findings in patients with interstitial cystitis. J Urol 153:290A

Sant G, Hanno PM (2001) Interstitial cystitis: current issues and controversies in diagnosis. Urology 57:82

Schnegelsberg B, Sun TT, Cain G et al (2010) Overexpression of NGF in mouse urothelium leads to neuronal hyperinnervation, pelvic sensitivity, and changes in urinary bladder function. Am J Physiol Regul Integr Comp Physiol 298:R534–R547

Seidel MF, Lane NE (2012) Control of arthritis pain with anti-nerve-growth factor: risk and benefit. Curr Rheumatol Rep 14(6):583–588

Suzuki M, Mizuno A, Kodaira K, Imai M (2003a) Impaired pressure sensation in mice lacking TRPV4. J Biol Chem 278:22664–22668

Suzuki M, Watanabe Y, Oyama Y, Mizuno A, Kusano E, Hirao A, Ookawara S (2003b) Localization of mechanosensitive channel TRPV4 in mouse skin. Neurosci Lett 353:189–192

Thorneloe KS, Sulpizio AC, Lin Z et al (2008) N-((1S)-1-{[4-((2S)-2-{[(2,4-dichlorophenyl)sulfonyl]amino}-3-hydroxypropanoyl)-1-piperazinyl]carbonyl}-3-methylbutyl)-1-benzothiophene-2-carboxamide (GSK1016790A), a novel and potent transient receptor potential vanilloid 4 channel agonist induces urinary bladder contraction and hyperactivity: part I. J Pharmacol Exp Ther 326:432–442

Vergnolle N, Cenac N, Altier C et al (2010) A role for transient receptor potential vanilloid 4 in tonicity-induced neurogenic inflammation. Br J Pharmacol 159:1161–1173

Vizzard MA (2000) Changes in urinary bladder neurotrophic factor mRNA and NGF protein following urinary bladder dysfunction. Exp Neurol 161:273–284

Vizzard MA (2001) Alterations in neuropeptide expression in lumbosacral bladder pathways following chronic cystitis. J Chem Neuroanat 21:125–138

Voets T, Talavera K, Owsianik G, Nilius B (2005) Sensing with TRP channels. Nat Chem Biol 1:85–92

Xu X, Gordon E, Lin Z, Lozinskaya IM, Chen Y, Thorneloe KS (2009) Functional TRPV4 channels and an absence of capsaicin-evoked currents in freshly-isolated, guinea-pig urothelial cells. Channels (Austin) 3:156–160

Yamada T, Ugawa S, Ueda T, Ishida Y, Kajita K, Shimada S (2009) Differential localizations of the transient receptor potential channels TRPV4 and TRPV1 in the mouse urinary bladder. J Histochem Cytochem 57:277–287

Yokoyama T, Kumon H, Nagai A (2008) Correlation of urinary nerve growth factor level with pathogenesis of overactive bladder. Neurourol Urodyn 27:417–420

Zvarova K, Vizzard MA (2005) Distribution and fate of cocaine- and amphetamine-regulated transcript peptide (CARTp)-expressing cells in rat urinary bladder: a developmental study. J Comp Neurol 489:501–517

Zvarova K, Murray E, Vizzard MA (2004) Changes in galanin immunoreactivity in rat lumbosacral spinal cord and dorsal root ganglia after spinal cord injury. J Comp Neurol 475:590–603